Structural Engineering and Mechanics, *Vol. 61, No. 5 (2017) 645-655*
DOI: https://doi.org/10.12989/sem.2017.61.5.645

Seismic applicability of a long-span railway concrete upper-deck arch bridge with CFST rigid skeleton rib

Changjiang Shao[*1], Jiann-wen Woody Ju[2,3a], Guoqing Han[4b] and Yongjiu Qian[1c]

[1]*School of Civil Engineering, Key Laboratory of Ministry of Education of Traffic Tunnel Engineering, Southwest Jiaotong University, Chengdu 610031, China*
[2]*Department of Civil and Environmental Engineering, University of California, Los Angeles, CA 90095, USA*
[3]*School of Civil Engineering, Southwest Jiaotong University, Chengdu 610031, China*
[4]*China Railway Eryuan Engineering Group Co. Ltd, Chengdu 610031, China*

(Received December 12, 2015, Revised November 6, 2016, Accepted December 6, 2016)

Abstract. To determine the seismic applicability of a long-span railway concrete upper-deck arch bridge with concrete-filled steel-tube (CFST) rigid skeleton ribs, some fundamental principles and seismic approaches for long-span bridges are investigated to update the design methods in the current Code for Seismic Design of Railway Engineering of China. Ductile and mixed isolation design are investigated respectively to compare the structural seismic performances. The flexural moment and plastic rotation demands and capacities are quantified to assess the seismic status of the ductile components. A kind of triple friction pendulum (TFP) system and lead-plug rubber bearing are applied simultaneously to regularize the structural seismic demands. The numerical analysis shows that the current ductile layout with continuous rigid frame approaching spans should be strengthened to satisfy the demands of rare earthquakes. However, the mixed isolation design embodies excellent seismic performances for the continuous girder approaching span of this railway arch bridge.

Keywords: seismic applicability; long-span railway arch bridge; CFST rigid skeleton; ductile design; seismic isolation; triple friction pendulum system; lead-plug rubber bearing

1. Introduction

Stiff structures are preferred for passenger dedicated lines to satisfy the higher serviceability limits compared with conventional railway bridge (Hu *et al*. 2014). A large number of world-class arch bridges have been constructed along the railways in China. For arch bridges crossing or near an earthquake-prone zone, seismic performances become the focus of attention. Further detailed studies should be done to find the seismic applicability of arch bridges with innovative structural designs. For example, the dynamic behavior and seismic performance of a long-span arch bridge with rigid skeleton ribs (made up of concrete-filled steel cubes and shaped-steel braces), continuous rigid frame, and T-type approaching spans should be researched.

The existing Code for Seismic Design of Railway Engineering of China (MR 2009) cannot keep up with the engineering requirement of large railway bridges. To adapt to the new demands of seismic design, the seismic code of railway engineering was revised to include ductile approach. Although the performance-based philosophies have been practiced by many codes (MT 2008, ATC-40 1996, Caltrans 2008), they are not yet executed systematically in the existing Code for Seismic Design of Railway Engineering of China (MR 2009). A practical example is that the seismic principles of special bridges, capacity-protected rules, strength and deformation check method and isolation design were elaborated clearly for long-span bridges in the existing codes (MT 2008, MHURC 2011). However, the above principles are not yet introduced into the existing railway engineering code. Further research on the design theory and methodology is required to analyze the possibility and applicability of the above principles in the future railway code. As a seismic design practice, we will attempt to adopt isolation and ductile design from other codes to optimize the seismic performances of a long-span railway arch bridge.

Ductile design is the most frequently used method to resist extensive earthquakes. In a ductile design, some members are permitted damage to prevent collapse of the capacity-protected members in a structure. Seismic isolation usually leads to less damage (almost elastic) in the isolated structures compared to ductile designed structures.

To improve the seismic applicability, a mixed layout of lead-plug rubber bearing and TFP has been employed to regularize the seismic demand of the arch bridge. Three independent pendulum mechanisms lead to different hysteretic characteristics at different motion stages of TFP (Morgan 2007, Morgan and Mahin 2008, 2011). Then the requirement of three-level seismic performance objectives

∗Corresponding author, Associate Professor
E-mail: shao_chj@126.com
[a]Professor
E-mail: juj@ucla.edu
[b]Engineer
E-mail: 66321544@qq.com
[c]Professor
E-mail: yjqian@sina.com

http://www.techno-press.org/?journal=sem&subpage=8
ISSN: 1225-4568 (Print), 1598-6217 (Online)

Table 1 Effective radii $\bar{R}_{eff}^{(i)}$ and friction coefficient $\bar{\mu}^{(i)}$ of different motion stages

Moving stage	Criteria of status	$\bar{R}_{eff}^{(i)}$ (m)	$\bar{\mu}^{(i)}$
Stage 1	$F^{(1)} \le F_{f1}$	$\bar{R}_{eff}^{(1)} = L_{eff2} + L_{eff3}$	$\bar{\mu}^{(1)} = \bar{\mu}_{eff2}^{(1)} + \bar{\mu}_{eff3}^{(1)}$
Stage 2	$F_{f1} < F^{(2)} \le F_{f4}$	$\bar{R}_{eff}^{(2)} = L_{eff1} + L_{eff3}$	$\bar{\mu}^{(2)} = \bar{\mu}_{eff1}^{(2)} + \bar{\mu}_{eff2}^{(2)} + \bar{\mu}_{eff3}^{(2)}$
Stage 3	$F^{(3)} = F_3 \le \dfrac{W}{L_{eff1}} d_1 + F_{f1}$	$\bar{R}_{eff}^{(3)} = L_{eff1} + L_{eff4}$	$\bar{\mu}^{(3)} = \bar{\mu}_{eff1}^{(3)} + \bar{\mu}_{eff2}^{(3)} + \bar{\mu}_{eff3}^{(3)} + \bar{\mu}_{eff4}^{(3)}$
Stage 4	$F^{(4)} = F_4 \le \dfrac{W}{L_{eff4}} d_4 + F_{f4}$	$\bar{R}_{eff}^{(4)} = L_{eff2} + L_{eff4}$	$\bar{\mu}^{(4)} = \bar{\mu}_{eff1}^{(4)} + \bar{\mu}_{eff2}^{(4)} + \bar{\mu}_{eff3}^{(4)}$
Stage 5	$u \le u_{max} = d_1 + d_2 + d_3 + d_4 + d_5$	$\bar{R}_{eff}^{(5)} = L_{eff2} + L_{eff3}$	$\bar{\mu}^{(5)} = \bar{\mu}_{eff2}^{(5)} + \bar{\mu}_{eff3}^{(5)}$

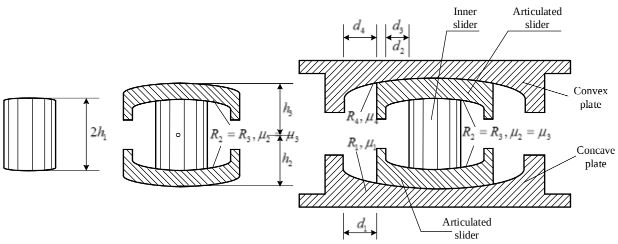

Fig. 1 Triple friction pendulum bearing

of railway engineering code can be satisfied (MR 2009). What is more important is that self-adaptive TFPs will endow the isolated bridge with selectable and controllable seismic objectives corresponding to different seismic demands under different levels of possible earthquakes.

2. Seismic design approach for long-span railway bridge

One of the efficient ways to reduce seismic response of a structural system is to increase damping. This is a fundamental design concept to dissipate the earthquake energy developed in the last several decades. It has to be regarded as a very attractive way to improve seismic resistance as both the natural period and the energy dissipation capacity are artificially increased. On the other hand, many structures are able to survive earthquakes by self-adaption escaping the frequency range where the seismic motion has greatest power, as a consequence of the period elongation due to accumulated damage of the components. The above two ways of seismic design are generally called isolation and ductile approaches for engineering structures.

2.1 Seismic isolation system

Seismic isolation is an approach of earthquake-resistance design based on the concept of reducing seismic demands rather than increasing earthquake resistance capacities of engineering structures. The purpose of isolation is to modify global response to improve structural performance (Priestley *et al*. 2007). The preferred isolation measures include friction pendulums devices and lead-plug bearings.

As one kind of promising innovative isolators, TFP systems are equipped with adjustable stiffness and damping alone according to the requirement of multilevel performance objective and fortification criterion, though it belongs to passive seismic device (Morgan 2007, Fenz and Constantinou 2008, Eröz and Roches 2008, Becker and Mahin 2013).

Here, R_1, R_2, R_3 and R_4 are radii of the slider surfaces (see Fig. 1). μ_1, μ_2, μ_3, μ_4 are the friction coefficients of slider 1, 2, 3 and 4. h_1 is half of the height of slider 1, h_2 is the height of the lower part under the mass center of slider 1 and 2, h_3 is the height of the upper part above the mass center of slider 1 and 2. To endow TFP with three levels of performance objectives needed by railway bridge, we assume that the curve surface 2 and 3 own the same radii and friction coefficients. That is $R_2=R_3$ and $\mu_2=\mu_3$. Then the effective radii of the spherical surfaces are $L_{eff1}=R_1-h_2$, $L_{eff2}=L_{eff3}=R_3-h_1=R_2-h_1$, $L_{eff4}=R_4-h_3$.

According to the mechanism of a TFP, the bearing force $F^{(i)}$ for the ith motion stage can be expressed as a function of displacement $u^{(i)}$ and the effective friction coefficient $\bar{\mu}^{(i)}$ of the ith slider

$$F^{(i)} = W\left(\frac{1}{\bar{R}_{eff}^{(i)}} + \bar{\mu}^{(i)}\right) \qquad (1)$$

Where, W is the weight of the upper structure above bearings. $\bar{R}_{eff}^{(i)}$ is the effective radius of the ith slider .

The effective radii, friction coefficients for different moving status of friction in Eq. (1) are shown in Table 1.

Where, $\bar{\mu}_{eff2}^{(1)} = \dfrac{\mu_2 L_{eff2}}{\bar{R}_{eff1}}$, $\bar{\mu}_{eff3}^{(1)} = \dfrac{\mu_3 L_{eff3}}{\bar{R}_{eff1}}$, $\bar{\mu}_{eff1}^{(2)} = \mu_1 \dfrac{L_{eff1} - L_{eff2}}{\bar{R}_{eff2}}$,

$\bar{\mu}_{eff2}^{(2)} = \dfrac{\mu_2 L_{eff2}}{\bar{R}_{eff2}}$, $\mu_{eff3}^{(2)} = \dfrac{\mu_3 L_{eff3}}{\bar{R}_{eff2}}$, $\bar{\mu}_{eff1}^{(3)} = \mu_1 \dfrac{L_{eff1} - L_{eff2}}{\bar{R}_{eff3}}$,

$\bar{\mu}_{eff2}^{(3)} = \dfrac{\mu_2 L_{eff2}}{\bar{R}_{eff3}}$, $\bar{\mu}_{eff3}^{(3)} = \dfrac{\mu_3 L_{eff3}}{\bar{R}_{eff3}}$, $\bar{\mu}_{eff4}^{(3)} = \dfrac{\mu_4 L_{eff4} - \mu_3 L_{eff3}}{\bar{R}_{eff3}}$,

$u^{(4)} = u + d_1\left(\dfrac{L_{eff2}}{L_{eff1}} - 1\right)$, $\bar{\mu}_{eff1}^{(4)} = \dfrac{L_{eff2} - L_{eff1}}{\bar{R}_{eff4}} \dfrac{d_1}{L_{eff1}}$, $\bar{\mu}_{eff2}^{(4)} = \dfrac{\mu_2 L_{eff2}}{\bar{R}_{eff4}}$,

$$\bar{\mu}_{eff\,3}^{(4)} = \frac{(\mu_4 - \mu_3) L_{eff\,3}}{\bar{R}_{eff\,4}}, \quad \bar{\mu}_{eff\,4}^{(4)} = \frac{\mu_4 L_{eff\,4}}{\bar{R}_{eff\,4}},$$

$$u^{(5)} = u - \frac{1}{\bar{R}_{eff\,3}}\left[d_1\left(1 - \frac{L_{eff\,2}}{L_{eff\,1}}\right) + d_4\left(1 - \frac{L_{eff\,3}}{L_{eff\,4}}\right)\right], \quad \bar{\mu}_{eff\,2}^{(5)} = \frac{\mu_2 L_{eff\,2}}{\bar{R}_{eff\,5}},$$

$$\bar{\mu}_{eff\,3}^{(5)} = \frac{\mu_3 L_{eff\,3}}{\bar{R}_{eff\,5}}.$$

The effective stiffness can be derived by the division of the current force and displacement, $k_{eff}^{(i)} = F^{(i)} / u^{(i)}$, corresponding to different kinematic stages. The effective period of the *i*th kinetic stage can be obtained as

$$T_{eff}^{(i)} = 2\pi \sqrt{\frac{1}{g\left(1/\bar{R}_{eff}^{(i)} + \bar{\mu}^{(i)}/u^{(i)}\right)}} \tag{2}$$

Attribute to the dynamic theory, the effective damping coefficient of the kinetic stage is

$$\xi_{eff_i} = \frac{2}{\pi} \frac{\bar{\mu}^{(i)}}{u^{(i)}/\bar{R}_{eff}^{(i)} + \bar{\mu}^{(i)}} \tag{3}$$

The above formulations form the theoretical framework to obtain the design parameters of a TFP bearing.

Since lead material yields in shear at relatively low stress and behaves approximately as an elastoplastic solid (Naeim and Kelly 1999), lead-rubber bearings have been adopted extensively since their introduction. Generally, the yielding levels of lead material are chosen so that the forces transmitted to other structural components are limited to their elastic, or low ductility, range. Therefore, most of the damages are concentrated in these dissipative devices with significant plasticization and possibly large residual displacements.

2.2 Ductile seismic design

Modern seismic design philosophy is to allow a structure to perform inelastically to dissipate the energy and maintain appropriate strength during severe earthquake attack (Park and Pauley 1974, Mander 1983, Chen *et al*. 2006, MT 2008, MHURC 2011). The philosophy of ductile design is to make usage of capacity-protected principle avoiding brittle failure modes. By introducing the seismic energy into the potential plastic hinge on the top or at the bottom of piers, most of the dynamic energy of ground motion can be dissipated by plastic deformations of ductile members. The hysteretic behaviors of ductile components provide energy dissipation to damp the response motion, which depends on the selection of longitudinal reinforcements, transverse bars and geometrical sizes of key sections.

To assess the seismic capacity of the key sections of a bridge, the anti-bending capacities are calculated. The transverse confining effect of concrete is considered by the modified formulation of compression strength (Mander *et al*. 1988). The overall performance of a bridge depends on the strength and deformation capacities of its individual components. When the ductile components experience a rare earthquake, there may be plastic deformations in these components. The ductile piers should be designed with enough deformation capacities such as plastic rotational angles. Here, the plastic rotations θ_p of ductile components are assumed to be smaller than the ultimate rotation capacity θ_u. The ultimate rotation can be calculated as (MHURC 2011)

$$\theta_u = L_p\left(\phi_u - \phi_y\right)/K \tag{4}$$

where L_p is the effective length of a plastic hinge, ϕ_u is the ultimate curvature, ϕ_y is the yielding curvature, K is the ductility coefficient of a structural component.

Through the above design measures, the ductile components can be prevented from collapsing with enough ductile capacity and avoiding brittle damage with adequate bearing capacity.

3. Validation of a railway arch bridge

As a practical example, ductile and isolation designs are implemented on a long-span railway arch bridge. If the ductile design measure cannot ensure excellent performance, the isolation design will be adopted to endow the system with rational seismic performances and self-adaptive flexibility.

According to the disaster report of 2008 Wenchuan Earthquake (Chen *et al*. 2012), the damage behaviors of these arch bridges include: collapse due to failed piers (Jingtianba Great Bridge), none seismic design (Nanba Great Bridge), partially serious damage in lateral braces and columns above ribs (Guixi Great Bridge, Tongziliang Bridge). The above disasters revealed certain types of bridges, which were designed without moderate seismic consideration based only on the traditional elastic design approach, are vulnerable to seismic disturbance. The similar failure can be found from the 1995 Hyogo-Ken Nanbu Earthquake. Five modern large steel-arch bridges and one old short RC-arch bridge were damaged (Yoshikazu and Hisahiro, 2004). The reported RC arch bridge suffered local compressive damage near the abutment and the top of arch. For the other five steel arch bridges, the superstructures were subject to minor damage, mostly on the bearings.

Based on the descriptions of seismic failures from arch bridges, some effective practical measures were proposed in the codes. Such as multi-box sections with large torsional rigidity and high integrity were selected. Rigid skeleton of concrete-fill steel tube was designed to reinforce the concrete arch ribs. These designs will be helpful to bear bend-press and torsional forces or their coupling behaviors under extensive earthquakes. The rigid skeleton aids in the construction of the arch rib with less shuttering investment compared with the conventional erection approach. This increases the spanning capability of the main arch. However, increasing spans leads to a problem on how to ensure seismic performances of these bridge in earthquake-prone regions. Comprehensive seismic designs should be executed on this class of bridges according to the structural characteristics and site properties.

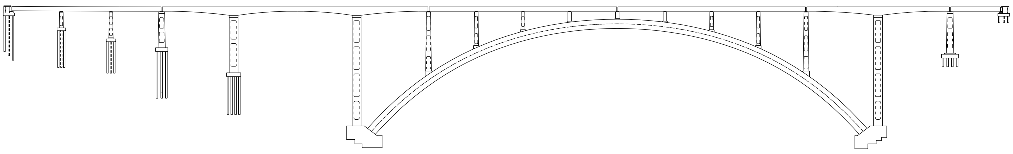

Fig. 2 Elevation graph of the arch bridge

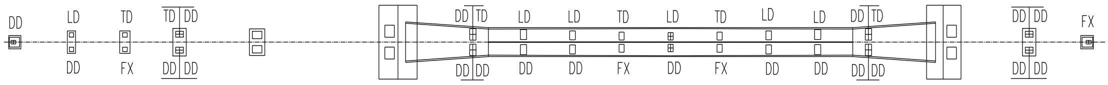

*DD denotes double-direction movable, LD longitudinal direction movable, TD transverse direction movable, FX fixed bearing.

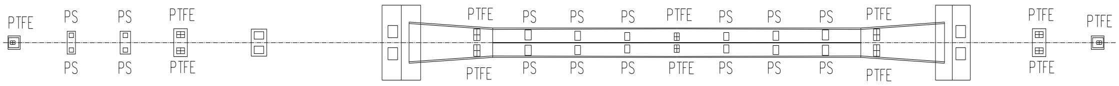

*PEFE denotes Teflon sliding bearing movable, PS denotes spherical steel bearing, TFP denotes triple friction pendulum.

Fig. 3 Layout of bearings

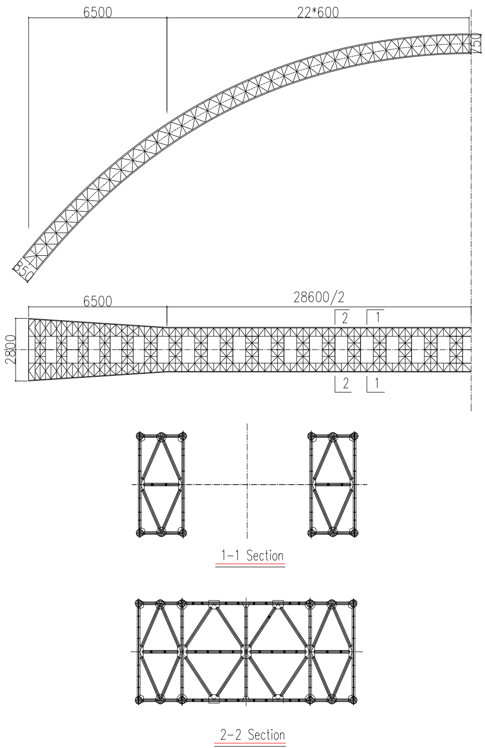

Fig. 4 Stiff skeleton by shaped-steel braces and concrete-filled steel tubes in arch rib

(a) Section

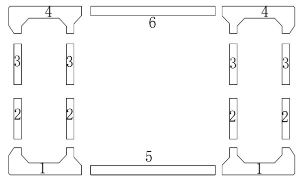

(b) Construction sequence

Fig. 5 Section and construction sequence number of the arch rib

3.1 Overview of the bridge

The span layout of the railway arch bridge is 3×42 m (continuous deck)+(60.9 m+104 m+60.9 m) (continuous rigid frame)+4×39.5 m (continuous deck)+4×39.5 m (continuous deck)+(60.9 m+60.9 m) (T-type rigid frame)+ 43.7 m (simply supported span=3.3 m, we refer to Fig. 2 below. The layout of the bearing type and the constraint direction is shown in Fig. 3. The decks above the arch rib are divided into two parts of continuous beam at the midspan. The main girder is made up of prestressed concrete box sections with vertical webs: cf. Fig. 4. The height of the girder and thickness of the bottom slab vary along a semi-cube parabolic curve in longitudinal direction of the bridge.

The arch rib is one of the most important load-bearing components in an arch bridge. It may undergo yielding deformation during a strong earthquake (Wakashima 2000, Alvarez *et al*. 2012). As one of the obvious structural properties, the box-section concrete rib is reinforced with stiff skeletons consisting of concrete-filled steel tubes and steel frames. This kind of structural design of arch rib will be helpful for the construction of the long-span concrete arch (Xie 2012). The second outstanding characteristic is that adjacent parts of the main span are continuous stiff skeleton on the left and T-frame bridge on the right other than continuous-deck layout as approaching spans: cf. Fig. 3. The third characteristic is the construction method of the arch rib, which is constructed in the sequence illustrated in Fig. 5. This constructing order will be helpful to decrease the effect of creep and shrink and unify the stress on box sections of the rib (Xie 2012).

The main part of the piers is made up of double columns with a thin-walled rectangular box section. The foundation

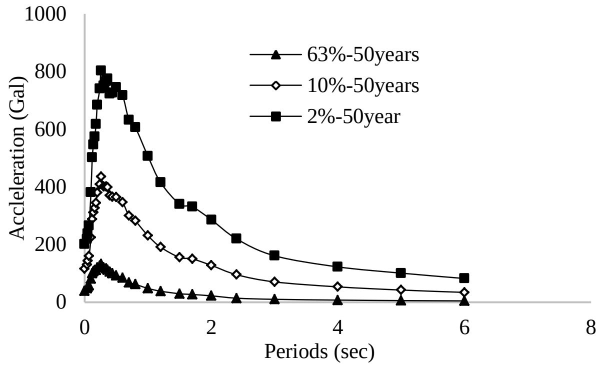

Fig. 6 Response spectra accelerations with a 5% damping ratio

is designed as cast-in-place drilled group piles with diameters from 1.25 m to 2.50 m. Figs. 4 and 5 show us part details of the structure.

3.2 Fortification criterion and ground motion of earthquake

The seismic fortification requires that the bridge should be equipped with different seismic performances under different levels of earthquake. The piers and piles of the bridge should be undamaged and remain elastic under rare major earthquakes. The three exceedance probabilities in the seismic risk report of the bridge site are: frequent earthquake with 63% exceedance probability (PGA 0.05 g), design earthquake with 10% exceedance probability (PGA 0.116 g) and rare earthquake with 2% exceedance probability (PGA 0.2 g) in 50 years. The input response spectra curves and the seismic ground motion history waves are represented in Fig. 6 and Fig. 7 respectively.

3.3 Performance objectives

According to the vulnerability and destructive risk, the performance objectives corresponding to the fortifications criteria are set up for different components based upon importance, reparability, replaceability and the reparable degree of difficulty post-earthquake. The most important load-bearing components, the arch rib, the foundation and the deck are difficult to be inspected, repaired and replaced after suffering seismic damages. These components shouldn't be damaged under a medium quake and should be repairable under a rare earthquake. They should remain elastic under the design seismic impact and are permitted to subject to repairable damage which would not adversely affect normal traffic in a short period. Further, the components can be repairable or replaceable after quake if their damages are controlled under specific extent, including the columns above the rib, the transferring piers, the piers of approach span, the lateral braces between the reinforcing frame of section steel and concrete-filled steel tube, the unseating prevention devices and the movement joints. They shouldn't be damaged under a minor earthquake, but should be repairable under a moderate quake and should not collapse under a rare seismic event.

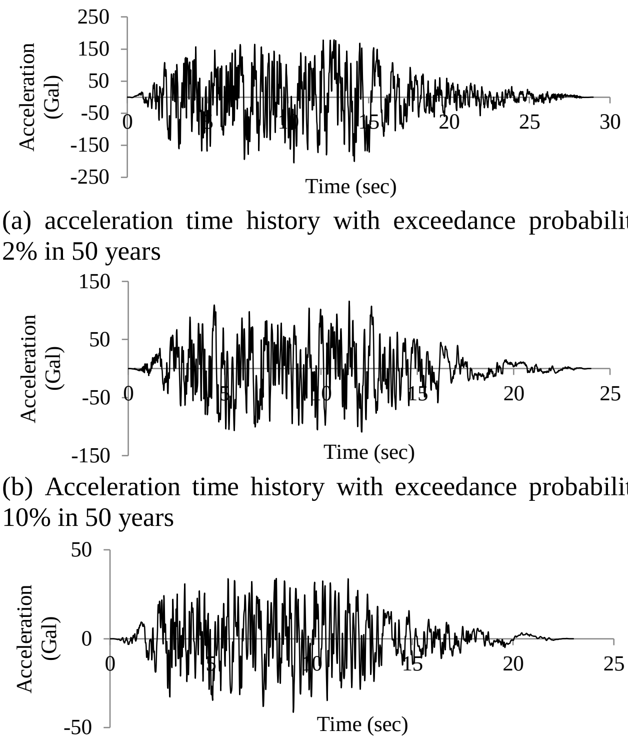

(a) acceleration time history with exceedance probability 2% in 50 years

(b) Acceleration time history with exceedance probability 10% in 50 years

(c) Acceleration time history with exceedance probability 10% in 50 years

Fig. 7 Acceleration histories of ground motions

When subjected to the seismic attack of a rare quake, the above components are allowed to suffer severe damage other than collapse.

The foregoing statements describe qualitatively the seismic performance objectives. The numerical analysis should be based on quantified objectives as presented in the next section. The performance objectives ensure continuous force-transferring paths and rational energy dissipation as well as appropriate collapse orders and paths. The structural seismic safety can be ensured through ductile design with adequate capacity and essential precondition of collapse prevention.

When ductile properties are included in the seismic design of concrete components, multi-level flexural strengths can be chosen as assessment criteria to assess the damage levels of fragile components. For the critical section of potential plastic hinge regions, the moment at the first yield of the outermost layer of longitudinal steel reinforcements is defined as M_y, the equivalent moment signified by M_{eq}, and the ultimate moment is M_u. The component is elastic when its moment is less than M_y, repairable when less than M_{eq}, and seriously damage other than collapse when less than M_u. The yielding, equivalent and ultimate moment can be acquired from a perfectly elastoplastic flexural-curvature curve (Caltrans 2008, MT 2008, MHURC 2011). As one critical component becomes plastic, sufficient deformation capacity should be ensured to prevent the structural system from collapse under rare earthquakes. Therefore, quantified performance objectives of ductile deformations should be rendered according to seismic fortifications.

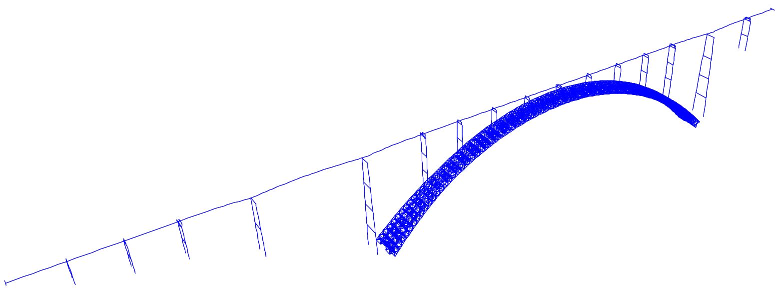

(a) Spatial view

(b) Vertical view

Fig. 8 Spatial and vertical view of structural FEM discretization

Table 2 No. of output key sections of the structural components

Output position	Section No.
Lowest hollow section of No. 4 pier	1
Lowest hollow section of No. 5 pier	2
Lowest hollow section of No. 1 pier above rib	3
Lowest hollow section of No. 4 pier above rib	4
Foot of rib	5

4. Numerical results

4.1 FEM model of structure

The 3D beam element is employed to establish the numerical model of an arch bridge; cf. Fig. 8. Although the rigid frame embedded in the rib section exerts little effect on the structural dynamic properties, it shares part of the loads sustained by the concrete rib. The rigid frame is simulated to reflect the real behaviors of the bridge despite of time-consuming calculation. The rib and stiff skeleton components share the same nodal joints to keep compatible deformation in the section of the arch. The steel spherical bearings are considered by elastoplastic links. The isolation devices are described by isolator elements of SAP2000. The interaction between piles and ground soil is considered by the elastic spring based on the M-method (MT 2007). The parameters of soil are obtained from the geotechnical investigation report of the engineering ground. The cushion cap is simplified as a rigid element with a lumped point mass. The static live load of a train and the secondary dead load are equivalent to line masses. The lateral diaphragms are simplified as to point masses. The coupling effects between the main bridge and approach span are included in the FEM model. The vertical excitation should be considered for this long-span arch bridge according to the Code for Seismic Design of Railway Engineering (MR, 2009). The output positions of structural responses are shown in Table 2. The fundamental period, 3.315s, corresponds to the out-of-plane bending of the bridge; the second dynamic mode is the longitudinal drift, and the vertical movement is given by the ninth mode.

4.2 Ductile design process

Ductile design are conventionally preferred to remain structural integrity at the cost of predicted structural damages. It is generally neither practical nor desirable to introduce plastic hinges in a superstructure. Plastic hinges of a column are typically chosen as the site for inelastic deformation. To ensure ductile flexural responses being achieved, it is essential that nonductile deformation should be inhibited. When the lateral reinforcements are designed inappropriately, the shear strength of a column will be less than the flexural strength. Once the initial shear strength is overcome and ideal flexural strength isn't achieved, the strength and stiffness will degrade rapidly. Therefore, it is necessary to ensure adequate margin of strength between the brittle failure modes and the designated ductile modes of deformation. Adequate transverse reinforcements should be provided in the region of potential plastic hinge to ensure nonductile failure modes occurring much later than ductile deformation.

In order to guarantee the minimum loss of life and property and keep ductile structural responses, a design should satisfy performance demands of seismic fortifications. The potential structural damages caused by earthquake beyond fortifications should be considered adequately. Accordingly, the damage sections and yielding orders of members are required by different strength levels. Through optimal design, the structure is endowed with adequate ductile capacity, requisite deformation and dissipative capacity.

The seismic flexural demands and capacities of critical pier sections are listed in Tables 3-4. The performance checks will certify that the structural or nonstructural components are not damaged when the demands are beyond the acceptable performance objectives.

The seismic demands of ductile and capacity-protected members increase intensely under rare earthquakes. The capacities of some critical sections cannot satisfy the seismic demands under lateral rare earthquakes. That means the transverse direction of arch bridges is more dangerous than the longitudinal direction under earthquake excitations (Usami *et al*. 2004). The similar conclusions were obtained by Alvarez *et al.* (2012). As large eccentric compression members, the load combination and the calculation results of the critical pier sections are exhibited in Table 4. The results show that the lateral seismic excitations exert greater

Table 3 Performance of key sections of original layout (under longitudinal & vertical excitations)

LC	OP	AF	FD	FC	RR
		P (kN)	M_y (kN·m)	M_y (kN·m)	(%)
Frequent quake	1	61375	4.17E+04	2.85E+05	0.62
	2	116916	1.37E+05	5.69E+05	0.81
	3	21777	3.09E+04	9.90E+04	1.09
	4	14221	5.51E+03	5.00E+04	0.75
	5	488218	2.42E+05	2.29E+06	0.76
Rare quake	1	51519	6.36E+05	3.23E+05	0.62
	2	97766	6.95E+05	6.35E+05	0.81
	3	13617	2.16E+05	1.10E+05	1.09
	4	7809	1.21E+04	5.44E+04	0.75
	5	366689	1.55E+06	2.34E+06	0.76

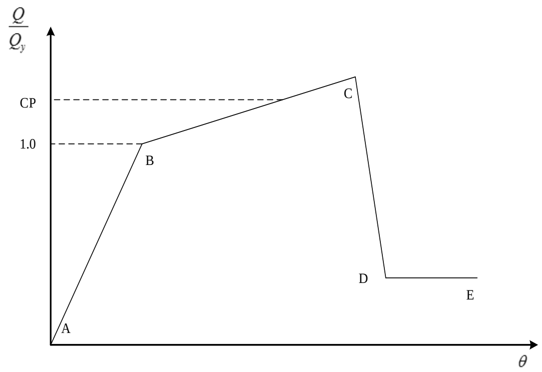

Fig. 9 Relationship of rotation and normalized forces due to earthquake

Table 4 Performance of key sections of original layout (under transverse & vertical excitations)

LC	OP	AF	FD		FC		RR
		P (kN)	M_y (kN·m)	M_z (kN·m)	M_y (kN·m)	M_z (kN·m)	(%)
Frequent quake	1	50582	1.23E+04	4.17E+04	2.54E+05	1.58E+05	0.62
	2	98000	9.18E+04	8.93E+04	5.16E+05	5.33E+05	0.81
	3	18777	2.34E+04	7.51E+03	9.29E+04	5.45E+04	1.09
	4	14405	2.60E+03	6.92E+03	5.03E+04	4.40E+04	0.75
	5	597826	6.49E+05	6.32E+05	2.84E+06	7.78E+06	0.76
Rare quake	1	-64498	1.01E+05	3.84E+05	--	--	0.62
	2	-137390	2.14E+05	7.97E+05	--	--	0.81
	3	-32926	6.12E+04	7.61E+04	--	--	1.09
	4	7158	5.16E+04	3.89E+04	5.35E+04	4.62E+04	0.75
	5	468254	9.70E+05	7.44E+06	2.74E+06	8.41E+06	0.76

Note, LC is the loading cases; OP is the output position; AF is the axial force; FD is the flexural demand; FC is the flexural capacity; Further, RR is the ratio of rebar.

Table 5 Ultimate rotation and status of key sections (under transverse & vertical excitations)

LC	OP	ϕ_p		ϕ_u		Status	RS	RR
		Y-axial (radian)	Z-axial (radian)	Y-axial (radian)	Z-axial (radian)	Stages	(%)	(%)
Transverse & vertical and Longitudinal & vertical	1	0.0007	0.0012	0.00834	0.00630	D to E	0.80	0.61
	2	0.0021	0.0012	0.00447	0.00515	B to C	0.80	0.81
	3	0.0011	0.00002	0.01149	0.00869	B to C	0.80	1.09

effects on seismic demands. The reason is that the transverse mass participation ratio is much larger than that in other directions. Some piers are tensioned intensely under the transverse rare earthquakes. This will result in serious reduction of seismic capacity of these concrete members. The enforcing measures should be provided to keep the structural performances acceptable under rare earthquakes.

To keep the balance between the seismic force and deformation demands of ductile components. The plastic rotation curvatures are calculated in the area of potential plastic hinges. The maximum plastic rotation curvature and the ultimate curvature are obtained to assess the seismic safety of these components (see Table 5). However, it can be found that the comparative results of ultimate rotations and plastic rotations of the key sections couldn't demonstrate the current status of the key members. Therefore the method of FEMA 356 (2000) is introduced to manifest the performance level of the vulnerable components, which is implemented in SAP2000 (see Fig. 9).

The curve in Fig. 9 could explained comprehensively as follows. The component will act elastically when the rotation is located between point A and B. As the load increases continuously, plastic deformations will appear in the member, causing the rotation beyond point B. If the rotation continues to increase but not greater than the value at point CP, the properties of components will suffer slight degradation. When the rotation is above point CP but below C, the components will be at the state of controllable weakness. However, if the increasing deformation is larger than that at point *C*, severe damage will appear in the structural components. Continuous high level seismic excitation will cause the members to collapse at the stage of DE. The current status of components can be found in Table 5.

The seismic performances of ductile designs are summarized in Table 6 with plastic hinge in the columns. The results illustrate that almost all the seismic capacities of these sections satisfy the demands of rare earthquakes. This suggests that seismic demand redistribution is rendered by plastic deformation of the key components due to intense ground motions. The softening behaviors dissipate the dynamic energy and reduce the responses of the key components.

The foregoing numerical results show that the higher economic investment is required for the ductile design to satisfy the demands of the rare earthquake. Specifically, under transverse rare earthquake, the higher demand requires the larger section size or much higher rebar ratio to ensure structural safety.

4.3 Analysis on isolated system

To reduce the in-plane inconsistent responses between the superstructure and the rib due to the structural irregularity (different height and stiffness of the piers),

Table 6 Performance of key sections of original layout (under transverse & vertical excitations)

LC	OP	AF	FD		FC		RR
		P (kN)	M_y (kN·m)	M_z (kN·m)	M_y (kN·m)	M_z (kN·m)	(%)
Rare quake	1	25922	5.02E+04	1.96E+05	3.56E+05	2.35E+05	0.62
	2	7598	1.98E+05	1.54E+05	2.42E+05	1.51E+05	0.81
	3	15040	3.18E+04	5.13E+04	6.80E+04	5.22E+04	1.09

Table 7 Geometric parameters of TFP device (m)

Parameter	R_1=R_4	R_2=R_3	h_1	h_2=h_3	d_1=d_4	d_2=d_3	L_{eff2}=L_{eff3}	L_{eff1}=L_{eff4}
Value	5.85	1.50	0.10	0.25	0.40	0.05	1.40	5.60

Table 8 Friction coefficients of TFP device

μ_2=μ_3		μ_1		μ_4	
min	max	min	max	min	max
0.01	0.02	0.02	0.06	0.06	0.12

Table 9 Assessment of design parameter of TFP bearing

Motion stage	$u_{\max}$ (m)	ξ_{eff}	k_{eff} (kN.m)	T_{eff} (sec)
Stage 1	0.11	0.212	24375	2.864
Stage 2	0.53	0.233	10263	3.817
Stage 3	0.56	0.377	12190	3.685
Stage 4	0.98	0.279	5688	5.674
Stage 5	1.00	0.067	8629	4.607

some effective measures should be adopted to regularize the structural properties. The most practical method is to weaken the stiffness of the connection between the ribs and the piers, such as dissipative bearings are located on the top of the piers. By this way, the effective stiffness and expected displacements of different piers are more similar to each other. Simultaneously, the seismic responses are reduced greatly by isolation device's weakening the coupling effects between the superstructure and substructure via the fundamental period elongation and the energy dissipation function (Naeim and Kelly 1999). To achieve the above sound effects, the continuous rigid-frame and T-frame spans are modified to a continuous girder system with the same geometric size as their original layout. The lead-plug rubber bearings are adopted on the intermediate piers of continuous deck spans. The TFP bearings are laid on the intermediate piers of the original stiff-frame and T-frame spans to optimize the seismic responses of a railway arch bridge. The steel spherical bearings are located on the transfer piers. This layout of bearings will help to realize regular and optimal structural performances. For this purpose, the isolation parameters should be investigated extensively according to the numerical simulation or even experimental study.

According the seismic requirements of the bridge, the geometric and physical parameters of TFP bearings are exhibited in Tables 7-8 respectively. The simplified mechanical coefficients (see Table 9) could be obtained from the foregoing formulations (2), (3). And the mixed layout of TFP and lead rubber bearings is shown Fig. 10.

The comparative numerical results between seismic ductile and isolation design (see Fig. 11) illustrate that the seismic demands decrease apparently. Then the section size and reinforcement needed are reduced substantially for isolation design. Therefore, seismic isolation measure is more efficient than ductile design to update the seismic performances of this bridge. The dissipative connection between the piers and deck is preferred for this type of long-span bridge. The comparison of dynamic axial forces and bending demands between ductile and isolation design demonstrate priority of the TFP design: adaptivity and multilevel performances.

The functional requirement of TFPs is to bear the shearing force transmitted from the foundation under earthquakes. Sufficient displacement capacities are needed to satisfy the maximum demands of seismic drifts. The displacement demands under three levels of earthquakes are list in Fig. 11. When the deformation capacity of the first stage is applied to satisfy the demands of Level-I earthquake, those of the second and third stage to satisfy the seismic demands of Level-II, and fourth and fifth stage for Level-III, it can be found that all the capacities cover all the earthquake demands. On the other hand, the design parameters in Tables 7-8 endow the isolated structure with adaptive seismic performances.

Great difference can be found among different levels of seismic displacements (see Fig. 11(a) and Fig. 11(b)) of bearings (output positions see Table 10). The above comparative numerical results show regularization of seismic requirements due to the adaptability of TFP devices with multi-level drift capacities based on three separate pendulum mechanisms. This property ensures seismic train-running comfort and safety by limiting the displacement

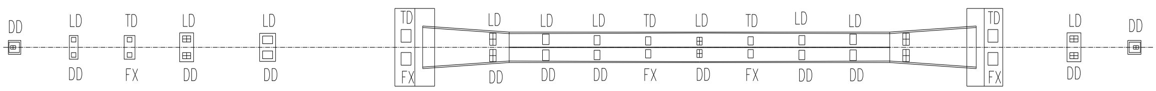

*DD denotes double-direction movable, LD longitudinal direction movable, TD transverse direction movable, FX fixed bearing.

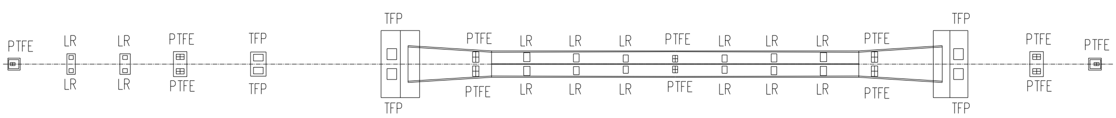

*PEFE denotes Teflon sliding bearing movable, PS denotes spherical steel bearing, TFP denotes triple friction pendulum.

Fig. 10 Layout of isolation bearings

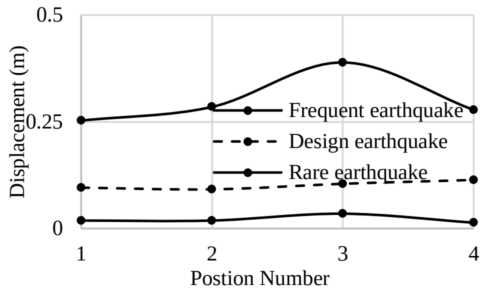

(a) Longitudinal drift demands of bearings

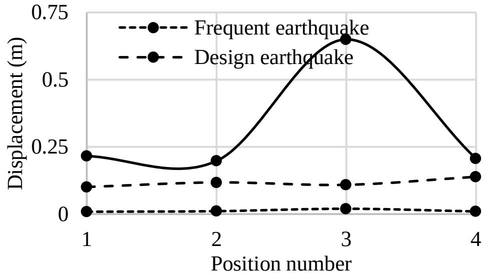

(b) Transverse drift demands of bearings

Fig. 11 Seismic drift demands of four positions under different level of earthquake

Table 10 Displacement output positons of bearings

Position Number	Output positions
1	Top of pier 4
2	Top of pier 5
3	Mid of M-span
4	Top of pier 6

Table 11 Displacement output positions of girder

Position number	Output positions
1	Top of left joint pier
2	Left of main girder
3	Medium of main span
4	Right end of main girder
5	Top of right joint pier
6	Arch crown

demand of operational period or mid-small earthquakes.

According to the results in Fig. 12(a), the internal force demands of the foot section of the arch rib are decreased by the isolation design. For example, the tensile forces of pier 4 and 5 are turned into pressure ones by isolators. At the same time, the moment demands of these sections are also reduced obviously in Fig. 12(b) and Fig. 12(c). That means the isolation design is effective to migrate seismic demands. The similar conclusions could also be obtained from the results in Fig. 13 and Fig. 14.

As far as the displacement demands of the girder are concerned, the key positions of the bridge are list in Table 11. The comparison of Figs. 13(a)-13(b) shows that the drift demands are amplified by isolators. However, those of arch crown are decreased due to isolation design.

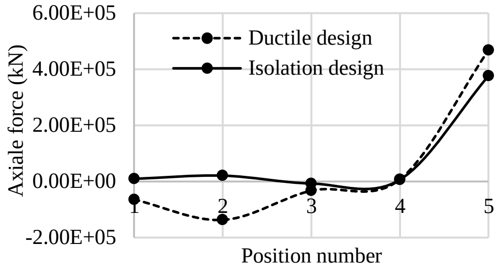

(a) Axial forces demands

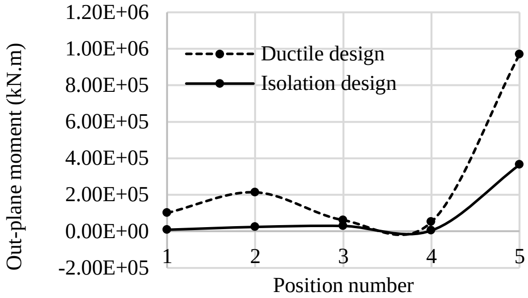

(b) In-plane ductile and isolation moment demands

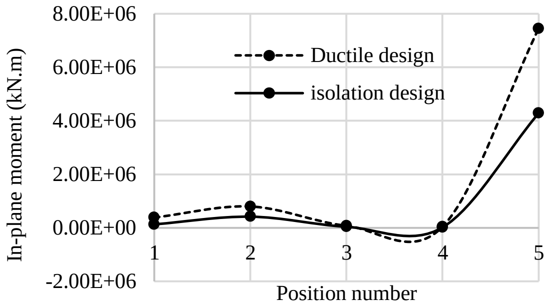

(c) Out-plane ductile and isolation moment demands

Fig. 12 Seismic internal force demands of key sections under rare earthquake

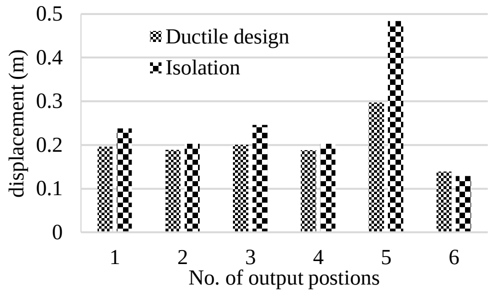

(a) Longitudinal displacement demand

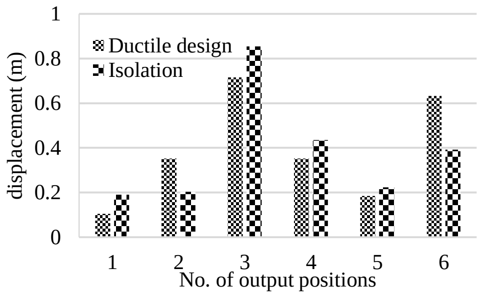

(b) Lateral displacement demand

Fig. 13 displacement demand of girder under rare earthquake (Unit: m)

5. Conclusions

According to the foregoing comparative analysis, some constructive conclusions should be obtained as follows:

- The original design of piers and columns above the arch rib should be strengthened to offer sufficient capacity to satisfy the demand of the potential ductile components under rare earthquakes. The final structural layout should balance the dilemma between the seismic safety and train-running comfort for the railway bridge.
- The flexural performances of key sections are investigated in the course of seismic design. However, other performances such as the shearing capacity of members and the displacement of bearings should also receive much attention. The different performance objectives should be optimized to ensure rational seismic structural response in accordance with the requirements of safety, functionality cost and even aesthetics.
- Comparative numerical results from ductile and isolation design show that the mixed layout of isolators endows the structural system with more excellent performances than the ductile design scheme. The seismic properties of the railway arch bridge are optimized substantially by lead-plug rubber bearings and TFP devices. Calculable and controllable bearing displacements can be obtained by changing the stiffness and damping of the system.
- Although the isolators are excellent enough to regularize the internal force demands under earthquakes, large seismic displacements should be considered for long-span railway bridges. In fact, excessively large drifts, especially the lateral displacement of the girder, caused by earthquakes may be hard to handle with for train-running safety and comfort in the process of design.
- More detailed researches are required to enhance the performance-based methodology for long-span railway bridges in the existing railway codes of China. The updated seismic design philosophy should be introduced to provide more robust and resilient structures and rational aseismic layout. Furthermore, innovative seismic design approaches should be developed to satisfy the engineering demand of long-span railway bridges.

Acknowledgments

The supports of the National Natural Science Fund Committee of China (Grant No. 51178395), Key Laboratory of Sichuan Province in Seismic Technology, (Grant No. SKZ2012006), Technological Research and Development Programs of the Railway Ministry of China (Contract No. 2010G018-A-1), and Technological Research and Development Programs of China Railway Engineering Group Company (Contract No. Key Project-12-2010) are gratefully acknowledged. Many thanks for Mr. Michael Borman (MTS Co. Ltd., USA) to help me to revised grammatical errors and upgrade readability of the essay.

References

Alvarez, J.J., Aparicio, A.C., Jara, J.M. and Jara, M. (2012), "Seismic assessment of a long-span arch bridge considering the variation", *Eng. Struct.*, **34**, 69-80.

Applied Technology Council (1996), ATC-40, Seismic evaluation and retrofit of concrete buildings, Red Wood City, California.

Becker, T.C. and Mahin, S.A. (2013), "Effect of support rotation on triple friction pendulum bearing behavior", *Earthq. Eng. Struct. Dyn.*, **42**, 1731-1748.

California Department of Transportation (2008), CALTRANS. CALTRANS Seismic Design Criteria Version 1.4. California.

Chen, L. (2012), *Seismic Damage Investigation of Wenchuan Earthquake-Bridges*, Renmin Jiaotong Press Co. Ltd, Beijing.

Chen, W.F. and Duan, L. (2006), *Bridge Engineering-Seismic Design*, CRC Press, Boca Raton.

Federal Emergency Management Agency (2000), FEMA 356, Prestandard and commentary for the seismic rehabilitation of buildings, Washington.

Fenz, D.M. and Constantinou, M.C. (2008), "Spherical sliding isolation bearings with adaptive behavior: Theory", *Earthq. Eng. Struct. Dyn*., **37**, 163-183.

Hu, N., Dai, G.L., Yan, B. and Liu, K. (2014), "Recent development of design and construction of medium and long span high-speed railway bridges in China", *Eng. Struct.*, **74**, 233-241.

Kawashima, K. and Mizoguti, A. (2000), "Seismic response of a reinforced concrete arch bridge", *12th World Conference on Earthquake Engineering*, Auckland, New Zealand.

Kitagawa, Y. and Hiraishi, H. (2004), "Overview of the 1995 Hyogo-ken Nanbu earthquake and proposals for earthquake mitigation measures", *J. JPN Associat. Earthq. Eng.*, **4**(3), 1-29.

Mander, J.B. (1983), "Seismic design of bridge piers", PhD Dissertation, University of Canterbury, Christchurch, New Zealand.

Mander, J.B., Priestley, M.J.N. and Park, R. (1988), "The theoretical stress-strain model for confined concrete", *J. Struct. Eng.*, **114**(8), 1804-1825.

Ministry of Housing and Urban-Rural Construction of People's Republic of China (MHURC) (2011), CJJ166-2011, Seismic Design Specification for Urban Bridge, Building Industrial Press Comp. Ltd. of China, Beijing.

Ministry of Railways of People's Republic of China (MR) (2009), GB 50111-2006, Seismic Design Specification for Railway Engineering, Plan Press Comp. Ltd. Of China, Beijing.

Ministry of Transportation of People's Republic of China (MT) (2008), JTG/TB02-01-2008, Seismic Design Guide of Highway Bridges, People's Transportation Press Comp. Ltd., Beijing.

Ministry of Transportation of People's Republic of China (MT) (2007), JTG D63-2007, Code for Design of Ground Base and Foundation of Highway Bridges and Culverts, People's Tranportation Press Comp. Ltd., Beijing.

Morgan, T.A (2007), "The use of innovative basis isolation systems to achieve complex seismic performance objectives", PhD Thesis, University of California, Berkeley, California, USA.

Morgan, T.A. and Mahin, S.A. (2008), "The optimization of multi-stage friction pendulum isolators for loss mitigation considering a range of seismic hazard", *The 14th World Conference on Earthquake Engineering*, Beijing, China.

Morgan, T.A. and Mahin, S.A. (2011), "The use of base isolation systems to achieve complex seismic performance objectives", University of California, Berkeley, PEER Report, 2011/06.

Murat, E. and Reginald, D.R. (2008)), "Bridge seismic response as a function of the Friction Pendulum System (FPS) modeling assumptions", *Eng. Struct.*, **30**, 3204-3212.

Naeim, F. and Kelly, J.M (1999), *Design of Seismic Isolated*

Structures: from Theory to Practice, John Wiley & Sons Ltd., New York, NY.

Priestley, M.J.N., Calvi, G.M. and Kowalsky, M.J. (2007), *Displacement-based Seismic Design of Structures*, IUSS Press, Pavia, Italy.

Usami, T., Lu, Z., Ge, H. and Kono, T. (2004), "Seismic performance evaluation of steel arch bridges against major earthquakes. Part 1: Dynamic analysis approach", *Earthq. Eng. Struct. Dyn*., **33**, 1337-1354.

Xie, H. (2012), "Study on structural type selection and mechanical behaviors of long-span railway concrete arch bridge with rigid skeleton", PhD Dissertation, Southwest Jiaotong University.

CC